

THE PHOTON COLLIDER AT ILC: STATUS, PARAMETERS AND TECHNICAL PROBLEMS*

V.I. TELNOV

Budker Institute of Nuclear Physics, Russian Academy of Sciences
Prospekt Lavrent'eva 11, 630090 Novosibirsk, Russia
telnov@inp.nsk.su

(Received April 12, 2006)

This paper is the second part of my overview on photon colliders given at the conference “The photon: its first hundred years and the future” (PHOTON2005 + PLC2005). The first paper V.I. Telnov, *The photon colliders: the first 25 years*, proceedings of PHOTON2005 and PLC2005, Warsaw and Kazimierz, Poland, 30 August–4 September 2005, volume 1, describes the first 25 years of the history and evolution of photon colliders. The present paper considers the photon collider at the ILC: possible parameters, technical problems and present status.

PACS numbers: 29.17.+w, 41.75.Ht, 41.75.Lx, 13.60.Fz

1. Introduction

There is a consensus in the particle-physics community that the next large project after the LHC should be a linear e^+e^- collider. Due to the high cost of such a collider it has been agreed to build a single collider at the energy $2E_0 = 0.5\text{--}1\text{ TeV}$ instead of the three regionally developed colliders, TESLA, NLC and JLC. In 2004, the International Linear Collider (ILC), based on the superconducting TESLA-like technology, was inaugurated. The project will be approved for construction after observation of interesting physics in this energy region by the LHC, which starts operation in 2007. At present, the development of the ILC and its detectors is proceeding under the guidance of the ILCSC, GDE and WWS committees. The next steps are: the choice of the baseline configuration, the reference design, site selection, and the conceptual and technical designs.

It is well understood that in addition to e^+e^- physics, linear colliders provide a unique opportunity to study $\gamma\gamma$ and γe interactions at high energy

* Presented at the PLC2005 Workshop, 5–8 September 2005, Kazimierz, Poland.

and luminosity [2–4]. High-energy photons are obtained by “conversion” of electrons into high-energy photons using Compton scattering of laser light at a small distance from the interaction point (IP), Fig. 1. The photon collider is highly appreciated by the physics community: more than 20% of all publications on linear colliders are devoted to photon colliders (in spite of the fact that at present this activity is not funded). The motivation for the photon collider is very strong:

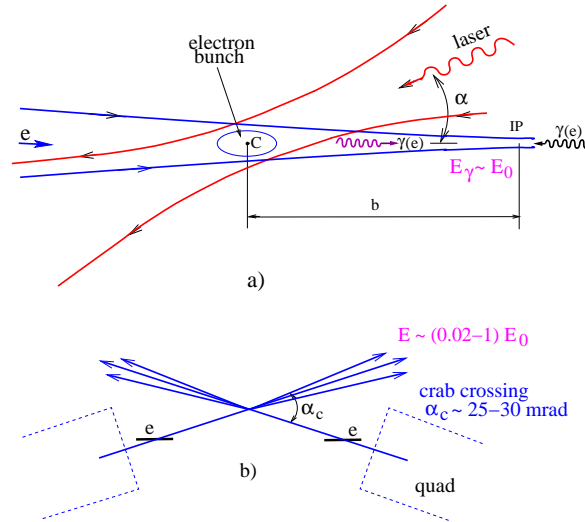


Fig. 1. Scheme of $\gamma\gamma, \gamma e$ collider.

- The physics is very rich [4–11]:
 - the energy is lower than in e^+e^- collisions only by 10–20%;
 - the number of interesting events is similar or even greater;
 - access to higher particle masses (single resonances in H , A , *etc.*, in $\gamma\gamma$, heavy charged and light neutral (SUSY, *etc.*) in γe);
 - in some scenarios, heavy H/A -bosons will be seen only in $\gamma\gamma$;
 - higher precisions for some important phenomena;
 - different (from e^+e^-) types of reactions;
 - highly polarized photons;
- there are no technical stoppers; the risk is small because in the case of technical problems the detector can continue taking data in the e^+e^- mode of collisions; the relative incremental cost is small;
- there is a great interest in the physics community to such experiments.

It is assumed that during the first several years of ILC operation all ILC detectors (whether one or two) will run in e^+e^- mode. Then, one of the interaction regions (IRs) and detectors will be modified for operation in the $\gamma\gamma, \gamma e$ mode. In other words, e^+e^- collisions are considered “baseline,” while $\gamma\gamma, \gamma e$ is seen as an “option”. Now, “option” is quite a misleading term, one that some people (including some of the ILC leaders) understand as an absolute priority of e^+e^- in all decisions and considerations, while the photon collider is seen as being far in the future and thus not requiring any attention at this time. Moreover, in order to reduce the ILC cost, there is a tendency to simplify the ILC design to a bare minimum: one IP, one detector, no options. One physicist’s comment regarding this was, “we do not need such a bicycle!”

Yes, the photon collider is part of the second stage of the ILC, but it has many specific features (see the list below) that strongly influence the baseline ILC configuration and the parameters of practically all of its subsystems. These requirements should be included into the baseline project from the very beginning — otherwise the upgrade from e^+e^- to $\gamma\gamma, \gamma e$ will be very costly (or even impossible at all) and (or) the parameters (such as the luminosity) of the photon collider will be much worse than in the case of a properly optimized design. All this means that **the photon collider should be considered from the beginning as an integral part of the ILC project!**

As for the cost, it is hard to imagine a project as cost-effective as the ILC photon collider. It practically doubles the ILC physics program while increasing the total cost project only by $\mathcal{O}(3\%)$. It is my firm belief that it will be no problem at all to convince the funding agencies that such a small increment of the ILC cost, which allows the ILC to study new phenomena in new types of collisions, is extremely well justified.

The next few years before the completion of the final ILC technical design are very important for the photon collider. All machine features required for the photon collider should be properly included in the basic ILC design. Of course, it is also important to continue the development of the physics program and to start, at last, the development of the laser system, which is a key element of the photon collider — but even more urgent are the accelerator and interaction-region aspects that influence the design of the entire ILC project.

The most comprehensive description of the photon collider available at present is part of the TESLA TDR [4]; almost all considerations done for TESLA are valid for the ILC as well. In the following sections I consider the most important problems of the photon collider that need special and careful attention of ILC designers.

2. Requirements for the ILC design

The photon collider imposes several special requirements that should be taken into account in the baseline ILC design:

- For the removal of disrupted beams, the crab-crossing angle at one of the interaction regions should be about 25 mrad; the ILC configuration should allow an easy transition between e^+e^- and $\gamma\gamma$ modes of operation.
- The $\gamma\gamma$ luminosity is nearly proportional to the geometric e^-e^- luminosity, so the product of the horizontal and vertical emittances should be as small as possible (this translates into requirements on the damping rings and beam-transport lines).
- The final-focus system should provide a beam-spot size at the interaction point that is as small as possible (compared to the e^+e^- case, the horizontal β -function should be smaller by one order of magnitude).
- The very wide disrupted beams should be transported to the beam dumps with acceptable losses. The beam dump should be able to withstand absorption of a very narrow photon beam after the Compton scattering;
- The detector design should allow easy replacement of elements in the forward region (<100 mrad).
- Space for the laser and laser beam lines has to be reserved.

Ignorance of any of these requirements can result in the future in a significant increase of the cost, in loss of time and in poor photon-collider parameters.

3. Photon collider luminosity

There are three luminosity problems at photon colliders: (1) obtaining high luminosities, (2) stabilization of beam collisions, (3) measurement of the luminosities, all these problems are discussed below. The most important and urgent at this time is the first problem.

3.1. Towards high $\gamma\gamma$, $\gamma\gamma$ luminosities

The $\gamma\gamma$ luminosity at the ILC energies is determined by the geometric luminosity of electron beams [4,12,13]. There is an approximate general rule: the luminosity in the high-energy part of the spectrum $L_{\gamma\gamma} \sim 0.1L_{\text{geom}}$, where $L_{\text{geom}} = N^2\nu\gamma/4\pi\sqrt{\varepsilon_{nx}\varepsilon_{ny}}\beta_x\beta_y$. So, to maximize the luminosity,

one needs the smallest beam emittances ε_{nx} , ε_{ny} and beta-functions at the IP, approaching the bunch length. Compared to the e^+e^- case, where the minimum transverse beam sizes are determined by beamstrahlung and beam instability, the photon collider needs a smaller product of horizontal and vertical emittances and a smaller horizontal beta-function.

The “nominal” ILC beam parameters are: $N = 2 \times 10^{10}$, $\sigma_z = 0.3$ mm, $\nu = 14100$ Hz, $\varepsilon_{nx} = 10^{-5}$ m, $\varepsilon_{ny} = 4 \times 10^{-8}$ m. Obtaining $\beta_y \sim \sigma_z = 0.3$ mm is not a problem, while the minimum value of the horizontal β -function is restricted by chromo-geometric aberrations in the final-focus system [4]. For the above emittances, the limit on the effective horizontal β -function is about 5 mm [14, 17]. The expected $\gamma\gamma$ luminosity $L_{\gamma\gamma}(z > 0.8z_m) \sim 3.5 \times 10^{33} \text{ cm}^{-2}\text{s}^{-1} \sim 0.17 L_{e^+e^-}$ (here the nominal $L_{e^+e^-} = 2 \times 10^{34} \text{ cm}^{-2}\text{s}^{-1}$) [14]. Taking into account the fact that many cross sections in $\gamma\gamma$ are larger than those in e^+e^- collisions by one order of magnitude, the event rate will be somewhat larger than in e^+e^- collisions.

The above-mentioned luminosity corresponds to the beam parameters optimized for the e^+e^- collisions where the luminosity is determined by collision effects. The photon collider has no such restrictions and can work with much smaller beam sizes. The horizontal beam size at the parameters under consideration is $\sigma_x \approx 300$ nm, while the simulation shows that the photon collider at such energies can work even with $\sigma_x \sim 10$ nm without fundamental limitations [4]. So, we are very far from the physical limit and should do all that is possible to minimize transverse beam sizes at the photon collider!

It should be noted that the minimum β_x depends on the horizontal emittance. It is about 5 mm for the nominal emittance and 3.7 (2.2) mm for emittances reduced by a factor of 2 (4), respectively. In the TESLA project, we considered emittances close to the latter case: $\varepsilon_{nx} = 0.25 \times 10^{-5}$, $\varepsilon_{ny} = 3 \times 10^{-8}$ m, which gives a $\gamma\gamma$ luminosity that is a factor of 3.5 higher!

The beams are produced in the damping rings (DR), so the minimum emittances are determined by various physics effects such as quantum fluctuations in synchrotron radiation and intra-beam scattering (IBS). The latter is the most difficult to overcome. Where is the limit? One of the possible way for reducing emittances is to decrease the damping time by adding wigglers [16], which has not yet been considered in detail by experts.

Damping rings are complex devices, so one should trust only careful studies. Nevertheless, I would like to make some rough estimates.

The equilibrium emittance in the wiggler-dominated regime due to quantum fluctuations [15]

$$\varepsilon_{nx} \sim 3.3 \times 10^{-11} B_0^3(\text{T})\lambda^2(\text{cm})\beta_x(\text{m}) \text{ m} . \tag{1}$$

The damping time

$$\tau_d = \frac{3m^2c^3}{r_e^2EB_0^2} = \frac{5.2 \times 10^{-3}}{E(\text{GeV})B_0^2(\text{T})} \text{sec.} \quad (2)$$

If wigglers fill 1/3 of the DR then for $B_0 = 2 \text{ T}$ and $E = 5 \text{ GeV}$ one gets $\tau = 7.5 \times 10^{-4} \text{ sec}$, which is more than 20 times smaller than the damping time in existing designs. For $\lambda = 10 \text{ cm}$ and $\beta_x = 5 \text{ m}$, the equilibrium normalized emittance due to synchrotron radiation is $\varepsilon_{nx} = 1.3 \times 10^{-7} \text{ m}$, which is 60 times smaller than the present nominal emittance. The vertical emittance will be much smaller as well. This does not take into account the IBS.

So, there appears to be a lot of room for decreasing the damping time and thus decreasing emittances in x and y , as well as β_x . Until β_x and σ_y are larger than their limits (σ_z and 1 nm, respectively), there is a strong dependence of the luminosity on emittances ($L \propto 1/\sqrt{\varepsilon_{nx}\varepsilon_{ny}\beta_x}$). The increase of the luminosity by a factor of 10 is not impossible with appropriate modifications to the damping rings! This would require more RF peak power, but that problem is solvable. The turn shift due to the beam space charge may be unimportant due to strong damping. This looks promising and needs a serious consideration by DR experts!

Let us assume a reduction (compared to the nominal beam parameters) of ε_{nx} by a factor of 6, ε_{ny} by a factor of 4 and β_x down to 1.7 mm (it is possible for such emittances). Then, one can have the following parameters of the photon collider: $N = 2 \times 10^{10}$, $\nu = 14 \text{ kHz}$, $\varepsilon_{nx} = 1.5 \times 10^{-6} \text{ m}$, $\varepsilon_{ny} = 1. \times 10^{-8} \text{ m}$, $\beta_x = 1.7 \text{ mm}$, $\beta_y = 0.3 \text{ mm}$, the distance between interaction and conversion regions is 1 mm, $\sigma_x = 72 \text{ nm}$, $\sigma_y = 2.5 \text{ nm}$, $L_{\text{geom}} = 2.5 \times 10^{35}$, $L_{\gamma\gamma}(z > 0.8z_m) \sim 2.5 \times 10^{34} \text{ cm}^{-2}\text{s}^{-1} \sim 1.25L_{e^+e^-, \text{nominal}}$.

The resulting $\gamma\gamma$ luminosity is greater than that at the ‘‘nominal’’ ILC beam parameters by a factor of 8.5. The statistics in $\gamma\gamma$ collisions would then be higher than in e^+e^- by one order of magnitude, which would open new possibilities such as the study of Higgs self-coupling in $\gamma\gamma$ collisions just above the $\gamma\gamma \rightarrow hh$ threshold [18, 19].

Figs. 2 show simulated luminosity spectra for these parameters. All important effects are taken into account, including the increase of the vertical beam size in the detector field due to the crab crossing (Sec. 3). In the figure on the right, only one of the electron beams is converted to photons, it is more preferable for γe studies due to easier luminosity measurement [21] and smaller backgrounds. The corresponding luminosity $L_{\gamma e}(z > 0.8z_m) \sim 2. \times 10^{34} \text{ cm}^{-2}\text{s}^{-1}$. By increasing the distance between the conversion and interaction regions, one can obtain a rather monochromatic luminosity spectrum of a reduced luminosity for the study of QCD processes [23].

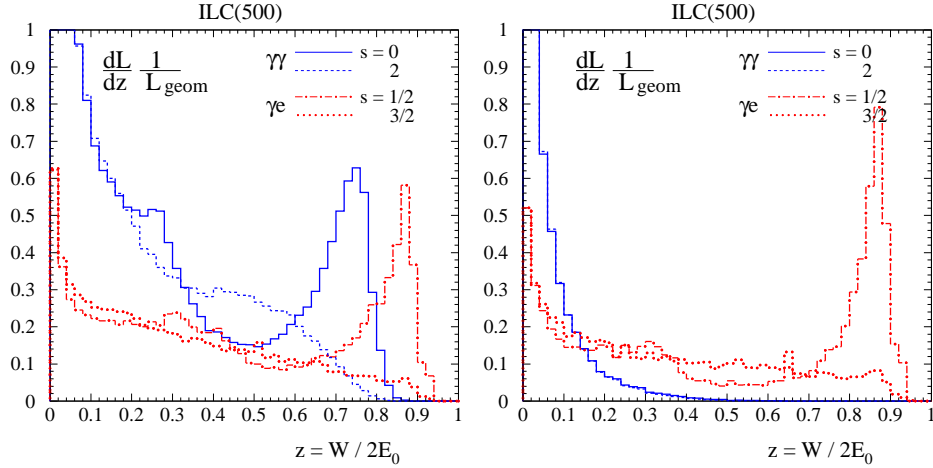


Fig. 2. $\gamma\gamma$, γe luminosity spectra. Left-hand side: both beams are converted to photons. Right-hand side: only one beam is converted to photons. See parameters in the text. $\gamma\gamma$.

I would like to stress once again that the parameters of the ILC damping rings are dictated not by e^+e^- , but by $\gamma\gamma$ collisions and a decision on the DR design should be based on the dependence $L_{\gamma\gamma} = f(\text{DR cost})$. It could be that the increase of the $\gamma\gamma$ luminosity by a factor of 8.5 as suggested above is too difficult, but even $\times 2$ to $\times 3$ improvement would be quite useful. This is very important and urgent question!

3.2. Luminosity stabilization

Beam collisions (luminosity) at linear colliders can be adjusted by a feedback system that measures the beam–beam deflection using beam position monitors (BPM) and corrects beam positions by fast kickers. This method is considered for e^+e^- collisions and is assumed for $\gamma\gamma$ as well [4].

There are some differences between the e^+e^- and $\gamma\gamma$ cases:

- In the e^+e^- case, at small vertical displacements the beams attract each other and oscillate. In the $\gamma\gamma$ case (e^-e^- as well), the beams repel each other; as a result, the deflection angle is larger.
- In the $\gamma\gamma$ case, due to Compton scattering, the average energy in the disrupted beam is several times smaller than the beam energy, which leads to a further increase of the deflection angle.
- In $\gamma\gamma$ collisions, σ_x is several times smaller than in the e^+e^- case. Due to a strong beam–beam instability, the kick is large and almost independent of the initial displacement.

There are two additional complications in $\gamma\gamma$ collisions:

- The deflection curves depend on the conversion efficiency.
- Due to the crossing angle, the disrupted beam is deflected (mostly vertically) by the detector field. This additional deflection is comparable to the beam–beam deflection angle and also depends on the conversion probability, see Fig. 5. This effect shifts the zero point and creates a problem for stabilization of beam–beam collisions.

Typical deflection curves for e^+e^- and $\gamma\gamma$ collisions are shown in Fig. 3. For the $\gamma\gamma$ case, a smaller energy is taken in order to emphasize the difference: the step-like behavior of the ϑ_y on the displacement Δ_y . More general cases for $\gamma\gamma$ are shown in Fig. 4.

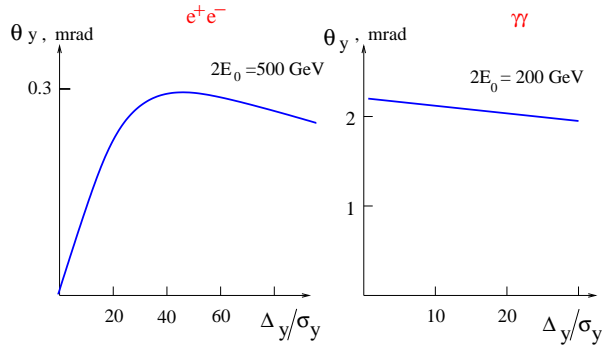


Fig. 3. Typical beam–beam deflection in e^+e^- and $\gamma\gamma$ collisions.

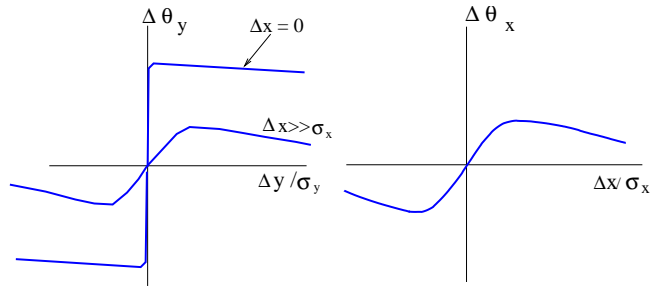


Fig. 4. Beam–beam deflections in $\gamma\gamma$ collisions.

We see that the deflection depends on the conversion coefficient, the deflection curves are symmetric but shifted vertically due to the detector field by some variable value.

How does one determine the vertical beam positions corresponding to the maximum $\gamma\gamma$ luminosity? Here is the sloution. All deflection curves $\theta_y = f(\Delta y)$ have one common feature: the derivatives f' reach the maximum at

the point of zero beam shifts where $L_{\gamma\gamma}$ is maximum. This is illustrated in Fig. 6: the width of this “resonance” curve is about $\pm 0.2\sigma_y$ (for the cases being considered).

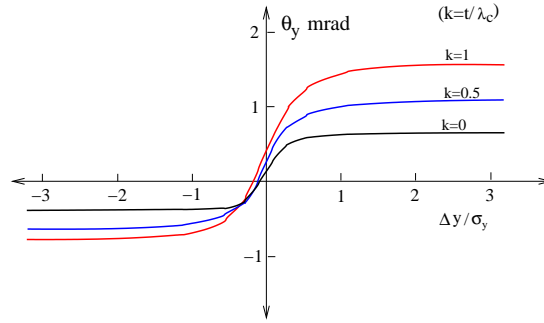


Fig. 5. Deflection curves in $\gamma\gamma$ collisions for various conversion efficiencies.

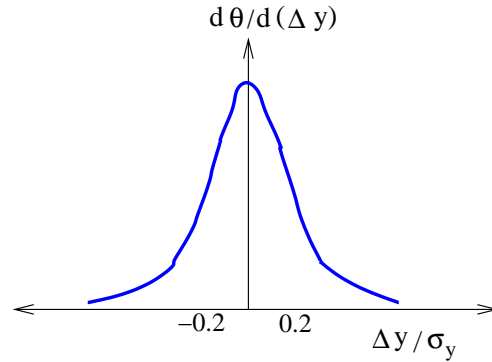


Fig. 6. Derivative of the typical deflection curve.

The recipe for the $\gamma\gamma$, γe luminosity stabilization is the following:

1. Varying Δy by decreasing steps (under software control), one finds the position of the jump in the deflection curve with an accuracy of about $2\sigma_y$.
2. Continue the scan with the step $0.1\sigma_y$ up and down around the point with the maximum derivative. The loss of $L_{\gamma\gamma}$ due to “walking” around the zero point will be negligibly small.
3. The horizontal zero point can be found in a similar way by varying the horizontal separation and measuring the horizontal deflection or by varying the horizontal separation and measuring the vertical deflection (the maximum vertical deflection corresponds to the zero horizontal separation).

4. In addition, the deflection in the detector field is very useful for optimization of the $e \rightarrow \gamma$ conversion. One just moves the laser beam and measures the vertical position of the outgoing beam in a BPM at a distance of about 4 m from the IP. The maximum beam displacement corresponds to the maximum conversion efficiency.

So, monitoring the beam–beam deflection is a good method of stabilization of the $\gamma\gamma$, γe luminosities at the ILC. The required algorithm does not appear to be difficult to implement thanks to the large train length and large inter-bunch spacing.

3.3. Luminosity measurement

The measurement of the luminosity at the photon collider is not an easy task. The spectra are broad and one should measure the luminosity and polarization as a function of energies E_1, E_2 of the colliding particles [21]. The luminosity spectrum and polarization can be measured using various QED processes. These are $\gamma\gamma \rightarrow l^+l^-$ ($l = e, \mu$) [4, 20, 21], $\gamma\gamma \rightarrow l^+l^-\gamma$ [21, 22] for $\gamma\gamma$ collisions and $\gamma e \rightarrow \gamma e$ and $\gamma e \rightarrow e^-e^+e^-$ for γe collisions [21]. Some other SM processes can be useful as well.

There is one unsolved problem in the measurement of linear polarizations in $\gamma\gamma$ collisions [24]. There exists an average linear photon polarization at a given energy that can be measured from the azimuthal distribution in $\gamma\gamma \rightarrow l^+l^-$. However, in addition to that, high energy photons have a linear polarization whose direction depends on the photon scattering angle. The directions of linear polarization of the colliding beams correlate, as the product of the linear polarizations $l_{1,\gamma}l_{2,\gamma}$ (which is presented in the cross section for the Higgs production) is quite large even for completely unpolarized initial particles. This correlation is not observable, neither in the cross section nor in the azimuthal distribution of the process $\gamma\gamma \rightarrow l^+l^-$. Fortunately, this effect is absent at the high-energy peak of $\gamma\gamma$ luminosity, which can be used for the Higgs study.

4. The crossing angle for the photon collider

4.1. Minimum crossing angle

The beam-crossing angle at the ILC is now one of the most hotly debated issues. For experimentation with e^+e^- beams, zero or small angles are preferable, but in this case there are some problems with the removal of used beams. At present, two IPs are considered for ILC, one with a small crossing angle, 2 mrad, and the other with a large crossing angle, 14 or 20 mrad, where 14 is somewhat more preferred.

In $\gamma\gamma$ collisions, the outgoing beams are strongly disrupted and for their removal a larger crossing angle is needed. In order to have better compatibility with e^+e^- this angle should be as small as possible. So, there are several questions:

- What is the minimum crossing angle suitable for $\gamma\gamma$?
- Is this angle compatible with e^+e^- ?
- What is the upgrade path from e^+e^- to $\gamma\gamma$?

For removal of these disrupted beams one needs the crab-crossing angle to be larger than the disruption angle plus the angular size of the final quad, see Fig. 1. There is an additional requirement: the field outside the quad should be small in order to add a small deflection angle for the low-energy particles in the outgoing beam.

After passing the conversion and collision points, the electrons have energy ranging from about 5 GeV up to E_0 and the horizontal disruption angle up to about 10 mrad, see Fig. 7 (due to limited statistics in simulation, about 10^5 macroparticles, the maximum angles should be multiplied by a factor of 1.2 [4]). Above this angle, the total energy of particles is less than that in the secondary irremovable e^+e^- background. The disruption angle for low-energy particles is proportional to $\sqrt{N/\sigma_z E}$ [25] and depends very weakly on transverse beam sizes.

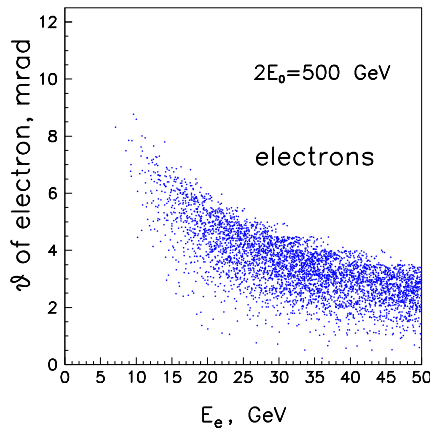


Fig. 7. Angles of disrupted electrons after Compton scattering and interaction with the opposing electron beam; $N = 2 \times 10^{10}$, $\sigma_z = 0.3$ mm.

Due to the crossing angle, the detector field gives an additional deflection angle to the disrupted beam, see Fig. 8. A crab-crossing angle of 25 mrad is assumed. These figures correspond to central collisions. For beams with an initial relative shift at the IP, the central core is shifted due to the instability

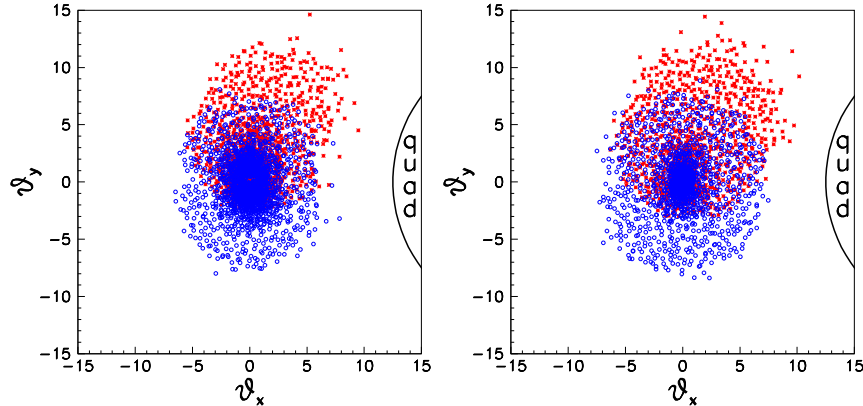


Fig. 8. The shift of the outgoing beam due to the detector field. Blue (square) points: only beam–beam deflection, red (stars) points: the detector field of 4 T is added. Positions of particles are taken at the distance of 4 m from the IP, at the place where they pass the first quad. Left-hand side figure: $2E_0 = 200$ GeV, right-hand side figure: $2E_0 = 500$ GeV.

of collisions but the maximum angles remain practically the same and decrease for large beams shifts. One can see that particles get mostly a vertical deflection, so the total vertical angle is about 17 mrad. The solenoid field also leads to some horizontal displacement (due to the vertical motion of particles) but it is smaller than the vertical shift of the beam.

A possible quad design for the photon collider was suggested by Parker [14, 26], see Fig. 9. The quad consists of two quads of different radii, one inside another, with opposite field directions. In this design, the gradient on

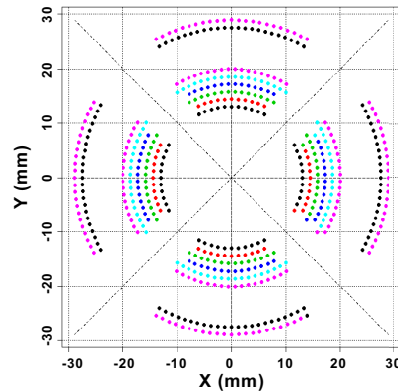


Fig. 9. The design principle of a superconducting quad (only the coils are shown). The radius of the quad with the cryostat is about 5 cm. The residual field outside the quad is negligibly small.

the axis is reduced only by 15%, and the field outside the quad is practically zero. The radius of the quad, the cryostat taken into account, is $R = 5$ cm. For the distance of the quad from the IP $L^* = 4$ m and the horizontal disruption angle of 12.5 mrad (10% margin), the minimum crab-crossing angle is $0.0125 + 5/400 = 25$ mrad. Obtaining the final numbers requires some additional checks.

Relative positions of the quad, the outgoing electron beam and the laser beams at the distance 4 m from the IP is shown in Fig. 10. We will return to this figure later when we consider the laser optics.

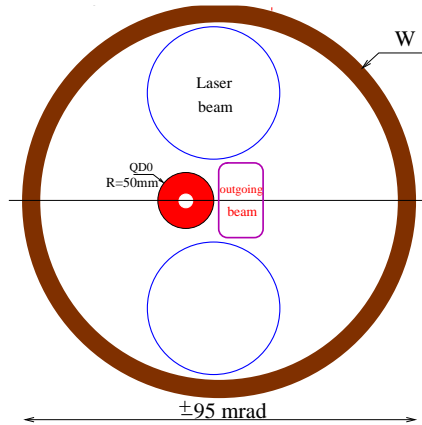


Fig. 10. Layout of the quad and electron and laser beams at the distance of 4 m from the interaction point (IP).

4.2. Other effects due to crossing angle

Crab-crossing. In order to preserve the luminosity at large crossing angles, the crab-crossing scheme is used, Fig. 1, where beams are tilted by special RF crab-cavities. The requirements on the time and amplitude stabilities of the RF become more stringent with the increase of the crab-crossing angle. This problem is more important for the photon collider where beams have smaller σ_x . For stabilization of the crab-crossing angle, a fast feedback should be used based on the rate of background processes (e^+e^- pairs) and the azimuthal distributions of outgoing particles (in the detector and beam dump), in addition to the beam stabilization feedback based on beam deflection (Sec. 3.2). This problem needs a detailed study.

Non-zero vertical collision angle. Due to the detector field, e^-e^- beams collide at a non-zero vertical collision angle that is several times larger than σ_y/σ_z , Fig. 11. This angle can be removed by a dipole correction winding in quads [27]. Such a correction shifts the IP vertically by about $300 \mu\text{m}$, which is an acceptable amount.

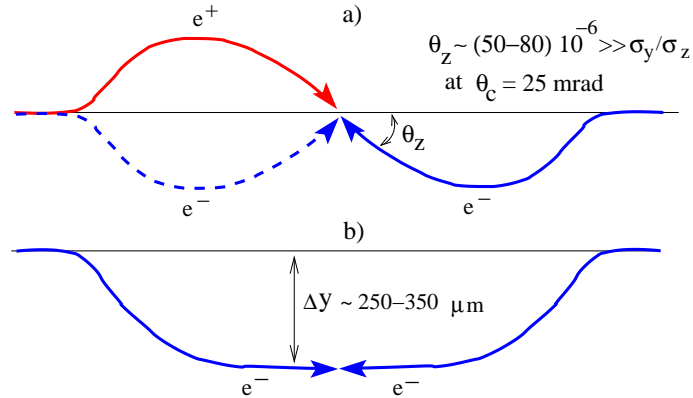


Fig. 11. Trajectories of electrons (positrons) in the presence of the solenoid field and a crab-crossing angle. At the lower figure, the e^-e^- collision angle is made zero using shifted quads.

The increase of the vertical beam size due to SR. Synchrotron radiation (SR) in the detector field leads to an increase of the vertical beam size. This effect was considered in Refs. [14, 27] for the detector fields as of Summer 2005. In Spring 2006, the length of the LDC detector was shortened from 7.4 m to 5.6 m. The simulation was repeated for the detector field presented in Fig. 12. Beam parameters correspond to the nominal ILC case: $2E_0 = 500$ GeV, $N = 2 \times 10^{10}$, $\sigma_z = 0.3$ mm, $\varepsilon_{nx} = 10 \times 10^{-6}$ m, $\varepsilon_{ny} = 0.04 \times 10^{-6}$ m, $\beta_x = 21$ mm, $\beta_y = 0.4$ mm.

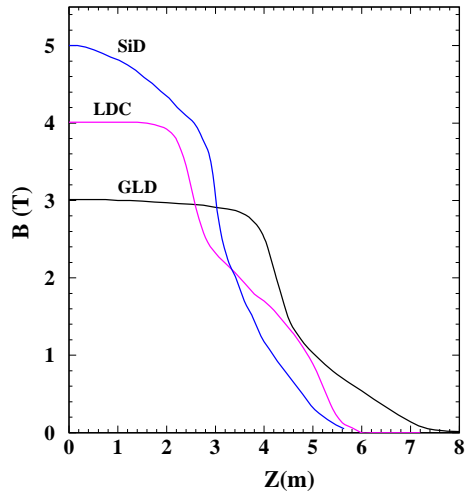


Fig. 12. Magnetic field $B(z, 0, 0)$ in LDC, SID and GLD detectors.

For the $\gamma\gamma$ case, instead of the $\gamma\gamma$ luminosity I simulated the e^-e^- luminosity (without the $e \rightarrow \gamma$ conversion) with $\sigma_y(\gamma\gamma) = \sqrt{2}\sigma_y(e^+e^-)$ in order to take into account an effective increase of the vertical beam size due to Compton scattering. All interactions between particles were switched off. The position of the first quad (shifted in the $e^-e^-(\gamma\gamma)$ case in order to have a zero collision angle) was $z = 3.8\text{--}6\text{ m}$ for all detectors. Results of the simulation are presented in Table I; the statistical accuracy is about $\pm 0.5\text{--}1\%$.

TABLE I

Results on $L(\alpha_c)/L(0)$.

e^+e^- collisions						
$\alpha_c(\text{mrad})$	0	20	25	30	35	40
LDC	1.	0.997	0.995	0.99	0.985	0.973
SID	1.	0.997	0.993	0.985	0.97	0.93
GLD	1.	0.995	0.99	0.98	0.96	0.935
$\gamma\gamma$ collisions						
$\alpha_c(\text{mrad})$	0	20	25	30	35	40
LDC	1	0.996	0.985	0.963	0.935	0.91
SID	1	0.994	0.99	0.98	0.955	0.93
GLD	1	0.998	0.993	0.985	0.973	0.94

It is interesting that LDC is the best for e^+e^- and the worst for $\gamma\gamma$, which is due to the compensation quadrupole in the $\gamma\gamma$ case. Its contribution depends on the shape of the field at the location of the quad (the radial field and the quad field have the same direction and, therefore, are added).

Conclusion: the crab-crossing angle of 25 mrad that is needed for the photon collider is compatible with e^+e^- .

4.3. Beam dump

The photon collider needs a special beam dump, one that is very different from the e^+e^- beam dump. There are two main differences:

- The disrupted beams at a photon collider consist of an equal mixture of electrons and photons (and some admixture of positrons).
- Disrupted beams at the photon collider are very wide (see Fig. 13), and need exit pipes of a large diameter.

- On the other hand, the photon beam following the Compton scattering is very narrow. At the distance of 250 m from the IP, the r.m.s. transverse size of the photon beam is $1 \times 0.35 \text{ mm}^2$, see Fig. 14, with a power of about 10 MW. It cannot be dumped directly at a solid or liquid material.

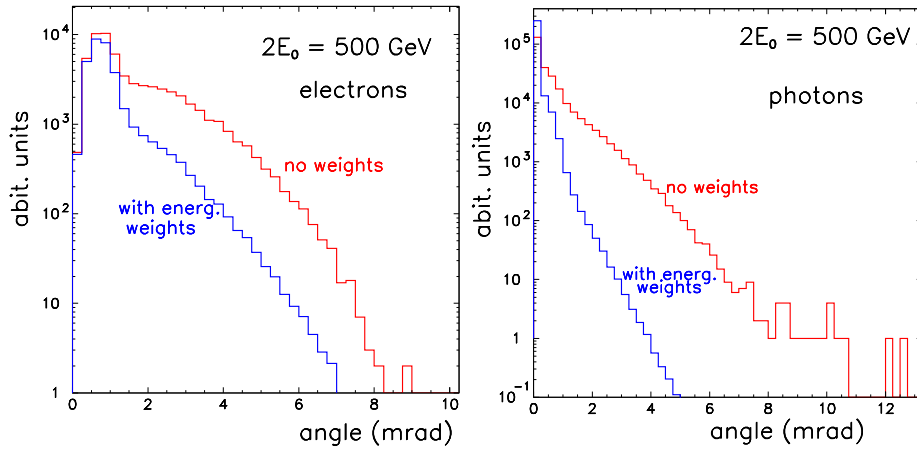


Fig. 13. Angular distributions of electrons (left-hand side) and photons (right-hand side) after the conversion and interaction points.

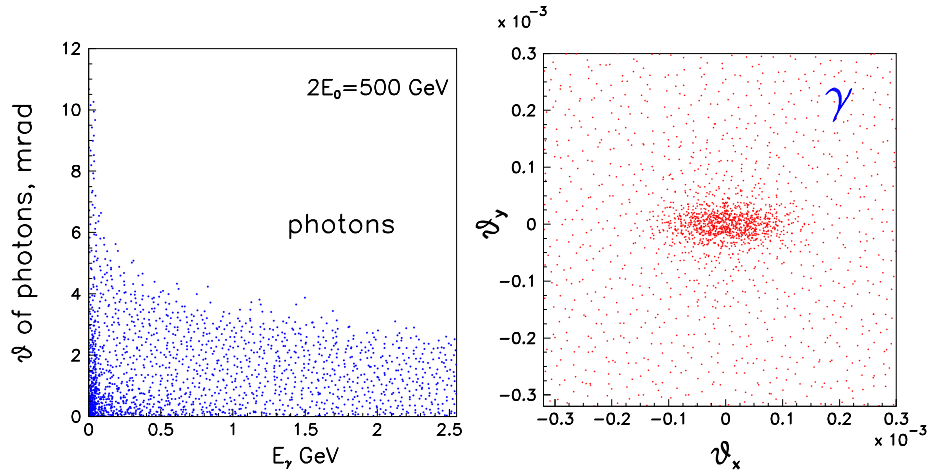


Fig. 14. Energy-angular distributions of beamstrahlung photons (left-hand side) and the angular distribution of Compton photons (right-hand side).

There exists an idea of such a beam dump, as well as some simulations [28], but a next step required, a more careful study. The idea is the following.

The water beam dump is situated at the distance of about 250 m from the IP, Fig. 15. The electron beam can be swept by fast magnets (as in the TESLA TDR) and its density at the beam dump will be acceptable. In order to spread the photon beam we suggest placing a gas target, for example Ar at $P \sim 4$ atm, at a distances of 120 to 250 m from the IP: photons would produce showers, the beam diameter would increase, and the density at the beam dump would become acceptable. In order to decrease the neutron flux in the detector, one can add a volume filled with hydrogen gas just before the Ar target, which would reduce the flux of backward-scattered neutrons at the IP at least by one order of magnitude. The corresponding numbers can be found in Ref. [28].

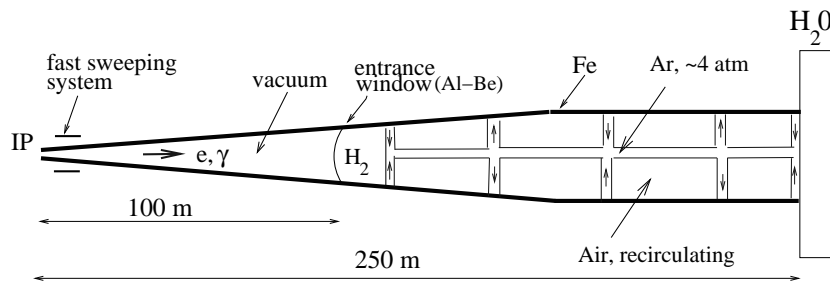


Fig. 15. An idea for the photon collider beam dump.

In order to reduce the diameter of the beamline between the beam dump and the IP, it is desirable to slightly focus the disrupted electron (positron) beam just after the exit from the detector (this issue has not been considered yet). The angular distribution of beamstrahlung photons is similar to that of beamstrahlung electrons that produced these photons. However, the energy of beamstrahlung photons produced by the rather low-energy large-angle electrons is only a small fraction of their energy, so the effective (energy-weighted) angular distribution of photons is narrower than that for electrons. According to Fig. 13 (right-hand side), for photons a clearance angle of ± 3 mrad will be sufficient, which is 75 cm at the distance of 250 m.

The Ar target should have a diameter of no more than 10 cm (a shower of such a diameter does not present a problem for the beam dump). The rest of the volume of the exit pipe with a diameter of about 1.5 m can be filled with air at 1 atm (or vacuum). Such measures are necessary in order to avoid unnecessary scattering of low-energy electrons traveling at large distances from the axis and thus to reduce the energy losses and activation of materials (water, air) in the unshielded area (it is difficult to shield a 200 m tube).

5. Configuration of the IP, transition from e^+e^- to $\gamma\gamma$

In order to save time and money, it is desirable to have an interaction region that requires a minimum modification for transition from e^+e^- to $\gamma\gamma$ collisions and back. The ideal case: the same beamlines and beamdumps, only minor modifications in the forward part of the detector. However, at present, the requirements presented by the e^+e^- and $\gamma\gamma$ cases are very different and no consensus reached. The differences are the following:

- $\gamma\gamma, \gamma e$: the crab-crossing angle is 25 mrad (minimum), the outgoing beams go straight to the beam dump. Beams are very disrupted, so only the simplest diagnostics is possible, such as measurement of the beam profile in the beam dump area;
- e^+e^- : the crab-crossing angle is 14–20 mrad, the extraction line includes many diagnostics such as precise measurement of the beam energy and polarization.

At present, the ILC beam delivery group has the following suggestion [29]. The extraction lines and the beam dump for e^+e^- and $\gamma\gamma$ are very different. Their replacements (transition to $\gamma\gamma$ and back after the energy upgrade) will be problematic due to induced radioactivity. Therefore, it makes sense to have different crossing angles and separate extraction lines and beam dumps for e^+e^- and $\gamma\gamma$. For the transition from e^+e^- to $\gamma\gamma$ one has to move the detector and about 700 m of the up-stream beamline, Fig. 16. The displacement of the detector is equal to 1.8 m and 4.2 m for the increase of the crab-crossing angle from 20 to 25 mrad and from 14 to 25 mrad, respectively.

I have an alternative suggestion: the same crossing angle, the same beam dump and no detector displacement. The cost will be reduced considerably, by hundreds of millions of dollars! No time is needed for the shift of beamlines (700 m!). What are disadvantages? In this case, the designs of the extraction line and the beamdump are dictated by $\gamma\gamma$, so no precision diagnostic in the extraction line for e^+e^- is possible. But is it really necessary? Indeed, without such special extraction line we can measure the energy and polarization before collisions, many characteristics during the beam collision (the acollinearity angles, distributions of the secondary e^+e^- pairs, the beam deflection angles); we can measure the angular distributions and the charged and neutral contents in the disrupted beams. All this allows the reconstruction of the dynamics of beam collisions, with a proper corrections in the simulation. For example, the depolarization during the collision is rather small, knowledge of beam parameters with a 10–20% accuracy is sufficient for introducing theoretical corrections. Direct measurement of the polarization after the collisions does not exclude the necessity of such a correction, it is just one additional cross check, but there are many other cross checks besides the polarization.

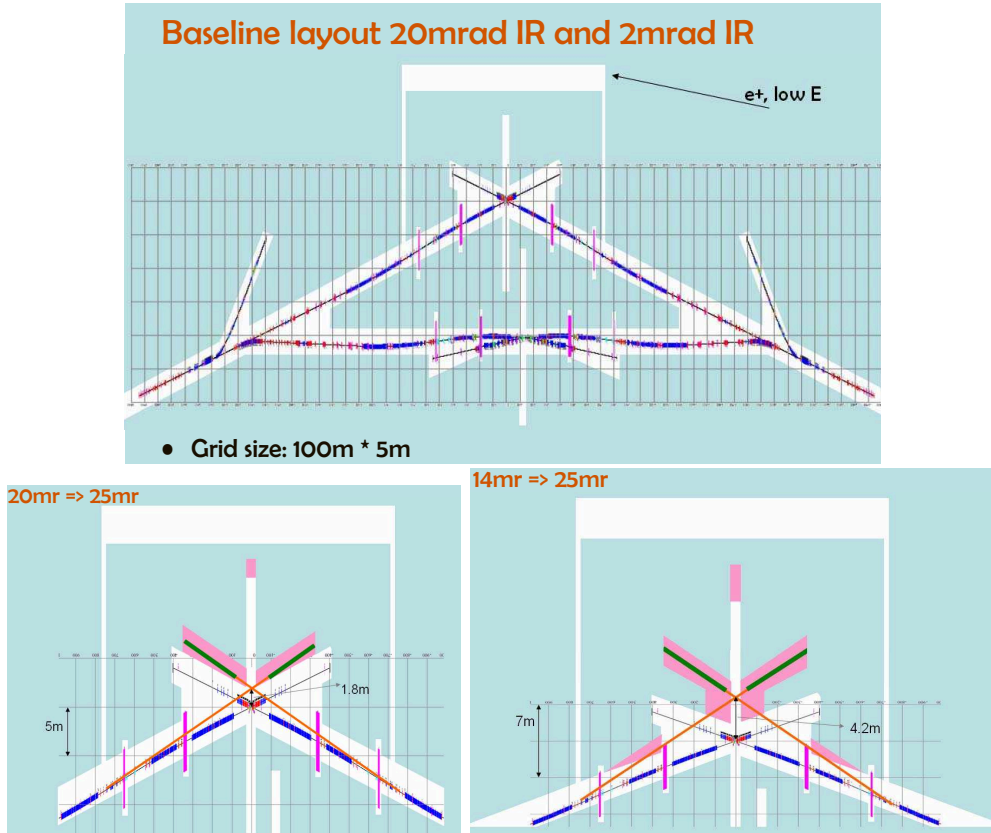


Fig. 16. Layout of the interaction regions at the ILC. The bottom figures show the upgrade path from e^+e^- to $\gamma\gamma$ according to [29]. See the author's alternative suggestion in the text below.

An additional remark. The requirement for the instrumented extraction line for e^+e^- restricts the accessible set of beam parameters and correspondingly the luminosity. One can not use it for the case of large beamstrahlung losses. It will not work, for example, in the CLIC environment or at the photon collider. In other words, such diagnostic of outgoing beams is useful but not absolutely necessary at linear colliders.

This suggestion is very attractive, cost- and time-effective, and deserves a serious consideration by appropriate GDE committees.

6. The laser system

The laser parameters required for the photon collider:

- Wavelength $\sim 1 \mu\text{m}$ (good for $2E_0 < 700 \text{ GeV}$);
- Time structure $c\Delta t \sim 100 \text{ m}$, 3000 bunches/train;

- Flash energy ~ 9 J (about one scattering length for $E_0 = 250$ GeV);
- Pulse length $\sigma_t \sim 1.5$ ps.

The most attractive scheme for a photon collider with the ILC pulse structure is storage and recirculation of a very powerful laser pulse in an external optical cavity [4, 12, 13, 30, 31]. This can reduce the required laser power by a factor of $Q \sim 100$ (Q is the quality factor of the cavity).

Dependence of the $\gamma\gamma$ luminosity on the flash energy and $f_{\#} = F/2R$ (flat-top laser beam) for several values of the parameter ξ^2 (which characterizes the multi-photon effects in Compton scattering, $\xi^2 < 0.3$ is acceptable [4]) is presented in Fig. 17 [14]. This simulation is based on the formula for the field distribution near the laser focus for flat-top laser beams. It was assumed that $\alpha_c = 25$ mrad and the angle between the horizontal plain and the edge of the laser beam is 17 mrad (the space required for disrupted beams and quads, see Fig. 10). At the optimum, $f_{\#} \sim 17$, or the angular size of the laser system is about $\pm 0.5/f_{\#} \approx \pm 30$ mrad. If the focusing mirror is situated outside the detector at the distance of 15 m from the IP, it should have a diameter of about 1 m. All other mirrors in the ring cavity can have smaller diameters, about 20 cm is sufficient from the damage point-of-view (diffraction losses require an additional check).

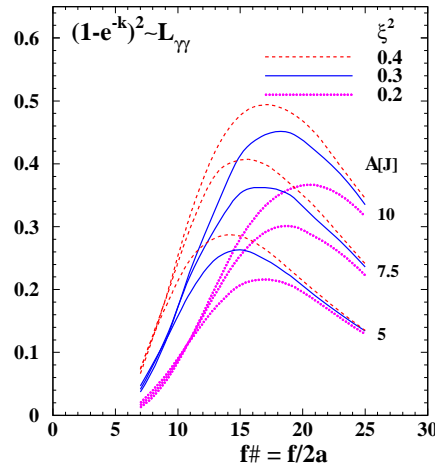


Fig. 17. Dependence of $L_{\gamma\gamma}$ on the flash energy and $f_{\#}$ (flat-top laser beam) for several values of the parameter ξ^2 .

The DESY-Zeuthen group has considered an optical cavity at the wave level, its pumping by short laser pulses, diffraction losses, *etc.* [31].

In the design with the final mirror located outside the detector, at a distance ~ 15 m from the detector center, the mirror's diameter is very large, about $d \sim 90$ cm, and the open angle in the detector as large as ± 95 mrad

is required. The detectors that are currently under consideration for e^+e^- have holes in the forward directions of about ± 33 – 50 mrad. Modifying the for $\gamma\gamma$ required that parts of ECAL, HCAL and the yoke be removable.

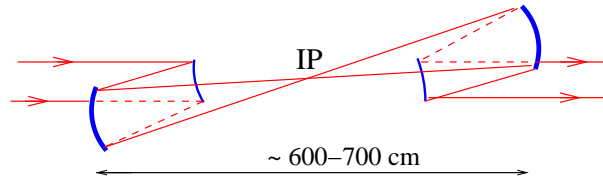


Fig. 18. Laser optics inside the detector.

An alternative scheme was considered in the TESLA TDR: the final pairs of mirrors are situated inside the detector, Fig. 18. In this case, the diameter of the focusing mirrors is only 20 cm and that of auxiliary mirrors is about 11 cm. The dead angle for tracking remains, as before, about ± 95 mrad; it can be smaller for the calorimeters, and may be the same as for e^+e^- . The laser density at the mirrors is far from the damage threshold, the average power is the most serious problem [4].

Though the cavity reduces substantially the required laser energy, the laser should still be very powerful. According to a LLNL estimation, the cost of one such laser is about \$10 M [32]. The photon collider needs two such lasers and one or two spares.

The same laser with the $1 \mu\text{m}$ wavelength can be used up to the ILC energy $2E_0 \sim 700$ GeV. At higher energies, the $\gamma\gamma$ luminosity decreases due to e^+e^- pair creation in the conversion region in collision of the high-energy and laser photons [3, 33] and due to the decrease of the Compton cross section, see Fig. 19 [14]. For the energy $2E_0 = 1$ TeV, the reduction in the luminosity due to this effect is about a factor of 2–3 compared to the

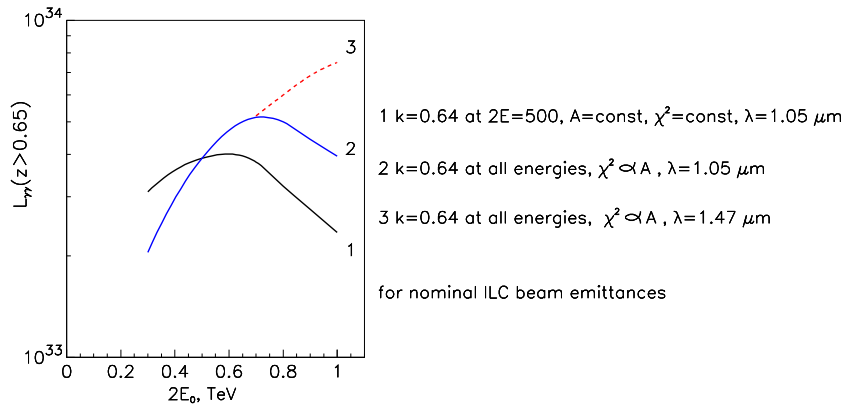


Fig. 19. Dependence of the $\gamma\gamma$ luminosity on the energy.

optimum case. For the high energies it is desirable to have a wavelength of about 1.5–2 μm . The technical feasibility of such a laser has not been studied yet.

7. Conclusion

In summary I would like to stress several important issues that need urgent attention of the ILC designers (GDE).

- We need a clear and inexpensive path from the e^+e^- to $\gamma\gamma$, γe modes of operation. The best would be an IP with a crab-crossing angle of about 25 mrad both for e^+e^- and $\gamma\gamma$. This is possible, but an effort is required to reach a consensus in the physics community. The presently suggested upgrade pass is too difficult, considerably increases the ILC cost and is time-consuming.
- In order to achieve high luminosity at the photon collider, damping rings with emittances that are much smaller than for e^+e^- are required. A serious and detailed study of this problem is needed. It is not excluded that a optimized wiggler-dominated storage ring will allow a $\times 3$ – $\times 5$ higher luminosity than that in the present design.
- The photon collider is not “an option” that can be implemented some time later — it is an integral part of the ILC project and considerably influences the baseline designs of practically all ILC systems. In addition, the key element of the project is a very unique, state-of-the-art laser system whose development required substantial time and finances. The photon collider can be successfully built only if it is an integral part of the e^+e^- , $\gamma\gamma$, γe , e^-e^- linear collider.

I would like to thank Maria Krawczyk for her great efforts on organization of PHOTON2005 in Warsaw and PLC2005 in Kazimierz and creating a beautiful and friendly atmosphere at the conferences.

REFERENCES

- [1] V.I. Telnov, *Acta Phys. Pol. B* **37**, 633 (2006).
- [2] I.F. Ginzburg, G.L. Kotkin, V.G. Serbo, V.I. Telnov, Preprint INP 81-50, Novosibirsk, Feb. 1981, in English; *Pisma ZhETF* **34**, 514 (1981); *JETP Lett.* **34**, 491 (1982).
- [3] I.F. Ginzburg, G.L. Kotkin, V.G. Serbo, V.I. Telnov, *Nucl. Instrum. Methods* **205**, 47 (1983) (Preprint INP 81-92, Novosibirsk, Aug. 1981, in English).

- [4] B. Badelek *et al.*, *Intern. Journ. Mod. Phys.* **A30**, 5097 (2004) [[hep-ex/0108012](#)].
- [5] E.E. Boos, *Nucl. Instrum. Methods* **A472**, 22 (2001) [[hep-ph/0009100](#)].
- [6] S. Brodsky, *Acta Phys. Pol. B* **37**, 619 (2006)[SLAC-PUB-11581].
- [7] M.M. Velasco *et al.*, proceedings of the APS/DPF/DPB Summer Study on the Future of Particle Physics (Snowmass 2001), eConf **C010630**, E3005 (2001) [[hep-ex/0111055](#)].
- [8] M. Krawczyk, *Eur. Phys. J.* **C33**, S638 (2004) [[hep-ph/0312341](#)].
- [9] A. De Roeck, DESY-04-123GF, DESY-PROC-2004-01F, Nov. 2003. Proceedings of the ECFA/DESY Study on Physics and Detectors at a Linear Collider, [[hep-ph/0311138](#)].
- [10] M.M. Muhlleitner, P.M. Zerwas, *Acta Phys. Pol. B* **37**, 1021 (2006), these proceedings;
- [11] F. Bechtel, G. Klamke, G. Klemz, K. Monig, H. Nieto, H. Nowak, A. Rosca, J. Sekaric, A. Stahl, DESY-06-007.
- [12] V.I. Telnov, *Nucl. Phys. Proc. Suppl.* **82**, 359 (2000) [[hep-ex/9908005](#)].
- [13] V.I. Telnov, *Nucl. Instrum. Methods* **A472**, 43 (2001) [[hep-ex/0010033](#)].
- [14] V.I. Telnov, proceedings of 2005 International Linear Collider Physics and Detector Workshop and 2nd ILC Accelerator Workshop, Snowmass, Colorado, 14–27 Aug. 2005 [[physics/0512048](#)].
- [15] H. Wiedemann, “*Particle Accelerator Physics: Basic Principles and Linear Beam Dynamics*”, Springer, Germany, Berlin 2003.
- [16] A. Wolski, talk at the Second ILC Accelerator Workshop, GG6 group, Snowmass, Colorado, August 14–27, 2005.
- [17] A. Seryi, talk at the Second ILC Accelerator Workshop, GG6 group, Snowmass, Colorado, August 14–27, 2005.
- [18] G.V. Jikia, *Nucl. Phys.* **B412**, 57 (1994).
- [19] R. Belusevic, G. Jikia, *Phys. Rev.* **D70**, 073017 (2004).
- [20] V.I. Telnov, Workshop on Physics and Exper. with Linear e^+e^- Colliders, Waikoloa, USA, *World Scientific*, 1993, p. 323.
- [21] A.V. Pak, D.V. Pavluchenko, S.S. Petrosyan, V.G. Serbo, V.I. Telnov, *Nucl. Phys. Proc. Suppl.* **126**, 379 (2004) [[hep-ex/0301037](#)].
- [22] V. Makarenko, K. Monig, T. Shishkina, *Eur. Phys. J.* **C32**, SUPPL1143-150 (2003) [[hep-ph/0306135](#)].
- [23] V.I. Telnov, Luminosity spectrum for study of gamma–gamma to hadron, http://www-h1.desy.de/maxfield/ggcol/montpellier_talks/Valery_lumispec_MONT1.PDF
- [24] V.I. Telnov, talk at the ECFA Workshop on Linear Colliders, Montpellier, France, 12–16 November 2003. http://www-h1.desy.de/maxfield/ggcol/montpellier_talks/Valery_polar_MONT2.PDF
- [25] V.I. Telnov, *Nucl. Instrum. Methods* **A294**, 72 (1990).

- [26] B. Parker, QDO external field compensation possibilities for gamma–gamma, talk at the Second ILC Accelerator Workshop, Snowmass, GG6 group, Colorado, August 14–27, 2005.
- [27] V.I. Telnov, talk at International Linear Collider Workshop (LCWS 2005), Stanford, California, 18–22 March 2005 [[physics/0507134](#)].
- [28] L.I. Shekhtman, V.I. Telnov, proceedings of the International Conference on Linear Colliders (LCWS 04), Paris, France, 19–24 April 2004 [[physics/0411253](#)].
- [29] A. Seryi, talk at the LCWS06, 9–13 March 2006, Bangalore, India <http://indico.cern.ch/contributionDisplay.py?contribId=207&sessionId=11&confId=568>.
- [30] I. Will, T. Quast, H. Redlin, W. Sandner, *Nucl. Instrum. Methods* **A472**, 79 (2001).
- [31] G. Klemz, K. Monig, I. Will, DESY-05-098 [[physics/0507078](#)].
- [32] G. Gronberg, talk at the Second ILC Accelerator Workshop, GG6 group, Snowmass, Colorado, August 14–27, 2005.
- [33] V.I. Telnov, *Nucl. Instrum. Methods* **355**, 3 (1995).